Inorg. Chem. **2005**, *44*, 5060–5067

Magneto–Structural Relationships in a Series of Dinuclear Oxalato-Bridged (Diphenyldipyrazolylmethane)copper(II) Complexes

Janet L. Shaw,[†] Gordon T. Yee,[‡] Guangbin Wang,[‡] David E. Benson,[§] Cagil Gokdemir,[§] and Christopher J. Ziegler*,[†]

Departments of Chemistry, University of Akron, Akron, Ohio 44325-3601, Virginia Polytechnic Institute and State University, Blacksburg, Virginia 24061, and Wayne State University, Detroit, Michigan 48202

Received December 16, 2004

A series of oxalato-bridged dinuclear copper(II) complexes of the general formula $[Cu_2(Pz_2CPh_2)_2(X)_2(\mu\text{-}C_2O_4)]$ ($X = Cl^-$ (**1**), NO_3^- (**2**), ClO_4^- (**3**); Pz_2CPh_2 = diphenyldipyrazolylmethane) or $[Cu_2(Pz^{3m}{}_2CPh_2)_2(H_2O)_2(\mu\text{-}C_2O_4)](NO_3)_2\cdot H_2O$ (**4**) ($Pz^{3m}{}_2CPh_2$ = diphenylbis(3-methylpyrazolyl)methane) was synthesized where the axial ligand was systematically varied to study its effect on structure and magnetic coupling. The structures of compounds **1**, **2**, and **4** have been elucidated by single-crystal X-ray diffraction. $[Cu_2(Pz_2CPh_2)_2(Cl)_2(\mu\text{-}C_2O_4)]$ and $[Cu_2(Pz_2CPh_2)_2(NO_3)_2(\mu\text{-}C_2O_4)]$ are isostructural and crystallize in the triclinic system, space group $P\bar{1}$, $Z = 2$, with $a = 8.6155(8)$ Å, $b = 10.1435(9)$ Å, $c = 11.3612(11)$ Å, $\alpha = 95.535(2)°$, $\beta = 110.303(2)°$, and $\gamma = 106.111(2)°$ for **1** and with $a = 8.863(7)$ Å, $b = 10.241(9)$ Å, $c = 11.425(10)$ Å, $\alpha = 98.985(14)°$, $\beta = 110.449(13)°$, and $\gamma = 103.664(14)°$ for **2**. $[Cu_2(Pz^{3m}{}_2CPh_2)_2(H_2O)_2(\mu\text{-}C_2O_4)]\cdot NO_3\cdot H_2O$ crystallizes in the monoclinic system, space group $C2/c$, $Z = 4$, with $a = 23.4588(14)$ Å, $b = 8.8568(5)$ Å, $c = 21.7818(13)$ Å, $\alpha = \gamma = 90°$, and $\beta = 100.8890(10)°$. Variable-temperature magnetic susceptibility studies indicate that all four compounds are strongly antiferromagnetically coupled ($2J/k = -364$, -344 cm^{-1} (**2**), -424 cm^{-1} (**3**), and -378 cm^{-1} (**4**)). Magnetic and EPR results are discussed with respect to structural parameters to explore possible magneto–structural correlations.

Introduction

Ligand-mediated coupling between paramagnetic metal centers continues to be an active area of investigation. The simplest of such systems occur when two d^1 or d^9 transition metal centers are coupled by a short bridging ligand.[1] Of the compounds that fit this description, dinuclear copper(II) compounds have been heavily examined, both synthetically and spectroscopically. Such complexes are relevant to dinuclear copper enzymes[2] including hemocyanin, an oxygen transport protein, and tyrosinase, an enzyme responsible for oxidation of phenolic substrates in certain organisms.[3] In addition, the magneto−structural analysis of bridged copper(II) complexes has received much attention in the literature due to its relevance to the spin frustration problem in copper-based superconductors.[4]

A very popular multiatom bridge for use in the synthesis of these compounds is the oxalate dianion (ox^{2-}). It is well-known that the oxalate ligand allows for magnetic communication between metal ions that can be greater than 5 Å apart.[5] However, with the elasticity of the copper(II) coordination environment and the multiple binding modes

* Author to whom correspondence should be addressed. E-mail: ziegler@uakron.edu.
[†] University of Akron.
[‡] Virginia Polytechnic Institute and State University.
[§] Wayne State University.

(1) Kahn, O.; Galy, J.; Journaux, Y.; Jaud, J.; Morgenstern-Badarau, I. *J. Am. Chem. Soc*. **1982**, *104*, 2165−2176.
(2) Lippard, S. J.; Berg, J. M. *Principles of Bioinorganic Chemistry*; University Science Books: Mill Valley, CA, 1994.
(3) Gamez, P.; Koval, I. A.; Reedijk, J. *Dalton Trans*. **2004**, 4079−4088.
(4) Seeber, G.; Kögerler, P.; Kariuki, B. M.; Cronin, L. *Chem. Commun*. **2004**, *14*, 1580−1581.
(5) (a) Gleizes, A.; Julve, M.; Verdaguer, M.; Real, J. A.; Faus, J.; Solans, X. *J. Chem. Soc., Dalton Trans.* **1992**, 3209−3216. (b) Geiser, U.; Ramakrishna, B. L.; Willett, R. D.; Hulsbergen, F. B.; Reedijk, J. *Inorg. Chem*. **1987**, *26*, 3750−3756. (c) Akhriff, Y.; Server-Carrió, J.; Sancho, A.; García-Lozano, J.; Escrivá, E.; Folgado, J. V.; Soto, L. *Inorg. Chem*. **1999**, *38*, 1174−1185. (d) Zhang, L.; Bu, W.; Yan, S.; Jiang, Z.; Liao, D.; Wang, G. *Polyhedron* **2000**, 1105−1110. (e) Núñez, H.; Timor, J.; Server-Carrió, J.; Soto, L.; Escrivà, E. *Inorg. Chim. Acta* **2001**, *318*, 8−14. (f) Smékal, Z.; Kameníèek, J.; Klasová, P.; Wrzeszcz, G.; ×b3indláø, Z.; Kopel, P.; _ák, Z. *Polyhedron* **2002**, 21, 1203−1209. (g.) Du, M.; Guo, Y.; Bu, X. *Inorg. Chim. Acta* **2002**, *335*, 136−140. (h.) Tuna, F.; Pascu, G. I.; Sutter, J.; Andruh, M.; Golhen, S.; Guillevic, J.; Pritzkow, H. *Inorg. Chim. Acta* **2003**, *342*, 131−138.

10.1021/ic048229t CCC: $30.25
Published on Web 06/15/2005

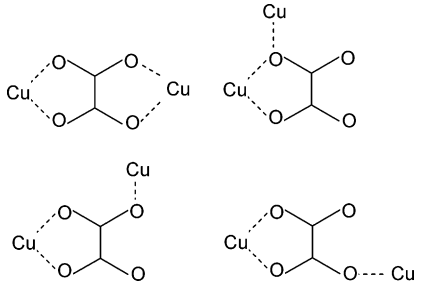

Figure 1. Selected binding modes of the oxalate dianion in dinuclear copper(II) compounds.[6]

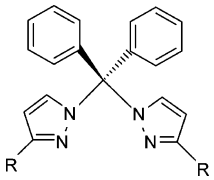

Figure 2. Diphenyldipyrazolylmethane (DPDPM), where R = H and Pz_2CPh_2 and R = CH_3 and $Pz^{3m}{}_2CPh_2$.

of the oxalate dianion come a plethora of possible symmetric and asymmetric geometries for resultant complexes. Figure 1 shows several of the observed binding modes of the oxalate dianion in dinuclear copper(II) compounds.

With regard to the degree of antiferromagnetic coupling between copper(II) centers, energies can range from 0 to −400 cm^{-1} depending on structural variations such as terminal ligand, coordination environment at the copper(II) ions, and bridging mode of the oxalate moiety. These structural factors are important in orienting the magnetic orbitals of the copper(II) ions for overlap with the oxalate σ-orbitals, which mediate the superexchange. The magnitude of antiferromagnetic coupling is directly related to the square of the overlap between magnetic orbitals centered on each copper(II) ion as mediated by the bridging oxalate.[7] Tuning magnetic coupling between the copper(II) ions continues to be of interest but is compounded by the degree of difficulty in controlling product formation and parametrizing structural effects.[8]

We have begun to explore the synthesis of copper(II) dinuclear oxalato-bridged complexes using the ligand diphenyldipyrazolylmethane (DPDPM) (Figure 2). Synthesized previously for use in polymerization catalysis,[9,10] this ligand is neutral and contains two pyrazole moieties available for bidentate metal ion coordination. We have found it useful for the synthesis of 1:1 metal to ligand complexes where the coordination environment at the copper center can be adjusted by modifying the peripheral pyrazole substitution.[11]

In this work we report the synthesis of four oxalato-bridged compounds where we have varied the copper(II) starting salt to study the effects of the axial ligand on geometry and temperature-dependent magnetic susceptibility. The complexes are of the general formula $[Cu_2(Pz_2CPh_2)_2(X)_2(\mu\text{-}C_2O_4)]$ (X = Cl^- (**1**), NO_3^- (**2**), ClO_4^- (**3**); Pz_2CPh_2 = diphenyldipyrazolylmethane) or $[Cu_2(Pz^{3m}{}_2CPh_2)_2(H_2O)_2(\mu\text{-}C_2O_4)](NO_3)_2{\cdot}H_2O$ (**4**) ($Pz^{3m}{}_2CPh_2$ = diphenylbis(3-methylpyrazolyl)methane), where the oxalate bridges in a symmetric bis(bidentate) fashion. Structural elucidation by single-crystal X-ray diffraction was possible for compounds **1**, **2**, and **4**, but only an isotropic solution of compound **3** was possible due to extensive twinning in the crystalline product. We are not reporting the final structure of compound **3** here, but the isotropic solution can be used to obtain geometric parameters for this complex. The degree of antiferromagnetic coupling is discussed in relation to several structural parameters measured from the crystal structures.

Experimental Section

Caution! *Perchlorate salts of metal complexes with organic ligands are potentially explosive. A small amount of material only should be prepared and it should be handled with care.*

All solvents and starting materials were obtained from commercial sources and were used without further purification. Syntheses of the ligands Pz_2CPh_2 and $Pz^{3m}{}_2CPh_2$ were reported previously.[11] Mass spectra were recorded using an ES MS Bruker Esquire-LC ion-trap mass spectrometer. The elemental analyses were performed on a CE440 analyzer at the School of Chemical Sciences Microanalysis Laboratory at the University of Illinois at Urbana-Champaign. Temperature-dependent magnetic susceptibility data were collected at Virginia Tech, and EPR data were obtained at Wayne State University. UV−visible spectra were obtained using a Hitachi U-3010 instrument.

Synthesis of $[Cu_2(Pz_2CPh_2)_2(Cl)_2(\mu\text{-}C_2O_4)]$ (1). $CuCl_2$ (0.091 g, 0.7 mmol) dissolved in CH_3OH/H_2O (5/10 mL) was added to a solution of Pz_2CPh_2 (0.201 g, 0.7 mmol) in CH_3OH (20 mL). The blue-green solution was allowed to stir for 30 min. To the reaction mixture was added $Na_2C_2O_4$ (0.045 g, 0.3 mmol). After the mixture was stirred for 24 h, a blue-green precipitate was collected by filtration and washed with H_2O (54% yield). Dissolving the precipitate in warm CH_3OH followed by slow evaporation of the solvent led to X-ray-quality crystals. IR (KBr): ν_{asy}(CO) 1640 cm^{-1}, ν_{sym}(CO) 1312 cm^{-1}, δ(O−C−O) 757 cm^{-1}. UV−vis (CH_3OH; λ/nm): 647 (1.28×10^2 M^{-1} cm^{-1}). ES MS (+ ion, CH_3OH): *m*/*z* 851.1 [M − Cl]. Anal. Calcd for $C_{40}H_{32}N_8Cl_2Cu_2O_4$ (M_r = 886.72): C, 54.18; H, 3.64; N, 12.63. Found: C, 53.29; H, 3.60; N, 12.13.

Synthesis of $[Cu_2(Pz_2CPh_2)_2(NO_3)_2(\mu\text{-}C_2O_4)]$ (2). $Cu(NO_3)_2$ (0.633 g, 3.4 mmol) dissolved in H_2O (30 mL) was added to a solution of Pz_2CPh_2 (1.015 g, 3.4 mmol) in CH_3OH (150 mL). The blue solution was allowed to stir for 30 min. To the reaction was added $Na_2C_2O_4$ (0.227 g, 1.7 mmol) dissolved in H_2O (20 mL). The solution was allowed to stir overnight resulting in a blue

(6) (a) Chaudhuri, P.; Oder, K. *J. Chem. Soc., Dalton Trans.* **1990**, 1597−1605. (b) Smékal, Z.; Thornton, P.; ×b3indláø, Z.; Klièka, R. *Polyhedron* **1998**, *17*, 1631−1635. (c) Gómez-Saiz, P.; García-Tojal, J.; Maestro, M.; Mahía, J.; Lezama, L.; Rojo, T. *Eur. J. Inorg. Chem.* **2003**, 2123−2132.
(7) Julve, M., Verdaguer, M.; Kahn, O.; Gleizes, A.; Philoche-Levisalles, M. *Inorg. Chem.* **1983**, 368−370.
(8) (a) Hay, P. J.; Thibeault, J. C.; Hoffman, R. *J. Am. Chem. Soc.* **1975**, *97*, 4884−4899. (b) Felthouse, T. R.; Laskowski, E. J.; Hendrickson, D. N. *Inorg. Chem.* **1977**, *16*, 1077−1089. (c) Kahn, O. *Inorg. Chim. Acta* **1982**, *62*, 3−14. (d) Julve, M.; Verdaguer, M.; Gleizes, A.; Philoche-Levisalles, M.; Kahn, O. *Inorg. Chem.* **1984**, *23*, 3808−3818. (e) Kahn, O. *Angew. Chem., Int. Ed. Engl.* **1985**, *24*, 834−850. (f) Cabrero, J.; Amor, N. B.; de Graff, C.; Illas, F.; Caballol, R. *J. Phys. Chem. A* **2000**, 104, 9983−9989.
(9) Shiu, K.; Yeh, L.; Peng, S.; Cheng, M. *J. Organomet. Chem.* **1993**, *460*, 203−211.
(10) Tsuji, S.; Swenson, D. C.; Jordan, R. F. *Organometallics* **1999**, *18*, 4758−4764.
(11) Shaw, J. L.; Cardon, T. B.; Lorigan, G. A.; Ziegler, C. J. *Eur. J. Inorg. Chem.* **2004**, 1073−1080.

precipitate that was removed by filtration and washed with H_2O and hexane (48% yield). Slow evaporation from a solution of warm CH_3OH or DMF produced X-ray-quality crystals. IR (KBr): ν_{asy}(CO) 1647 cm^{-1}, ν_{sym}(CO) 1312 cm^{-1}, δ(O−C−O) 755 cm^{-1}, (NO_3^-) 1384 cm^{-1}. UV−vis (CH_3OH; λ/nm): 670 (1.39×10^2 M^{-1} cm^{-1}). ES MS (+ ion, CH_3OH; *m*/*z*): 878.2 [M − NO_3], 407.9 [M − $2NO_3$]. Anal. Calcd for $C_{40}H_{32}N_{10}Cu_2O_{10}\cdot C_3H_7NO$ (M_r = 1012.82): C, 50.99; H, 3.89; N, 15.21. Found: C, 51.39; H, 3.77; N, 15.36.

Synthesis of $[Cu_2(Pz_2CPh_2)_2(ClO_4)_2$ (μ-$C_2O_4)]$ (3). $Cu(ClO_4)_2\cdot 6H_2O$ (1.204 g, 3.2 mmol) was dissolved in H_2O (25 mL) and added to a solution of Pz_2CPh_2 (0.984 g, 3.3 mmol) in CH_3OH (100 mL). The solution turned deep blue and was allowed to stir for 30 min. To the reaction a solution of $Na_2C_2O_4$ (0.219 g, 1.6 mmol) in H_2O (25 mL) was added. After the mixture was stirred for 1 h, a blue precipitate formed, which was removed by filtration and washed with H_2O and hexanes (74% yield). Crystals can be grown from warm acetonitrile layered with H_2O, but the quality of the crystals is poor due to extensive twinning. All attempts to grow suitable crystals for X-ray structural elucidation resulted in twinned morphologies that were not suitable for anisotropic solutions. IR (KBr): ν_{asy}(CO) 1654 cm^{-1}, ν_{sym}(CO) 1320 cm^{-1}, δ(O−C−O) 749 cm^{-1}, (ClO_4^-) 1120, 1071, 1056 cm^{-1}. UV−vis (CH_3OH; λ/nm): 679 (1.16×10^2 M^{-1} cm^{-1}). ES MS (+ ion, CH_3OH; *m*/*z*): 915.1 [M − ClO_4], 407.9 [M − $2ClO_4$]. Anal. Calcd for $C_{40}H_{32}N_8Cl_2Cu_2O_{12}$ (M_r = 1014.82): C, 47.34; H 3.18; N, 11.04. Found: C, 47.31; H, 3.09; N, 11.09.

Synthesis of $[Cu_2(Pz^{3m}{}_2CPh_2)_2(H_2O)_2$ (μ-$C_2O_4)](NO_3)_2\cdot H_2O$ (4). $Cu(Pz^{3m}{}_2CPh_2)(NO_3)_2$[11] (0.766 g, 1.5 mmol) in H_2O (30 mL) was combined with a solution of $Na_2C_2O_4$ (0.099 g, 0.7 mmol) in H_2O (10 mL). A blue precipitate formed immediately, which was removed by filtration and washed with additional H_2O (51% yield). Dissolving the precipitate in warm CH_3OH followed by slow evaporation of the solvent led to X-ray-quality crystals. IR (KBr): ν_{asy}(CO) 1654 cm^{-1}, ν_{sym}(CO) 1309 cm^{-1}, δ(O−C−O) 763 cm^{-1}. UV−vis (CH_3OH; λ/nm): 702 (1.24×10^2 M^{-1} cm^{-1}). ES MS (+ ion, CH_3OH; *m*/*z*): 934.2 [M − $2H_2O$ + NO_3], 435.9 [M − $2H_2O$]. Anal. Calcd for $C_{44}H_{44}N_8Cu_2O_6\cdot 2NO_3\cdot H_2O$ (M_r = 1049.99): C, 47.34; H 3.18; N, 11.04. Found: C, 47.31; H, 3.09; N, 11.09.

X-ray Crystallography. The X-ray intensity data for compounds **1**−**4** were measured at 100 K (Bruker KRYO-FLEX) on a Bruker SMART APEX CCD-based X-ray diffractometer system equipped with a Mo-target X-ray tube (λ = 0.710 73 Å) operated at 2000 W power. Crystals were mounted on a cryoloop using Paratone N-Exxon oil and placed under a stream of nitrogen. The detector was placed at a distance of 5.009 cm from the crystals. Frames were collected with a scan width of 0.3° in ω. Analyses of the data sets showed negligible decay during data collection. The data were corrected for absorption with the SADABS program. The structures were refined using the Bruker SHELXTL software package (version 6.1) and were solved using direct methods until the final anisotropic full-matrix, least-squares refinement of F^2 converged.[12] Experimental details for all of the structures are provided in Table 3.

EPR Spectroscopy. EPR spectra were recorded on a Bruker ESP-300 X-band EPR spectrometer. Analyses were performed in the solid state using 0.01% (w/w) silica mixtures. All spectra were collected at 105 K using the following parameters: microwave power, 50 mW; microwave frequency, 9.43 GHz (confirmed by TEMPO standard[13]); modulation frequency, 100 kHz; modulation amplitude, 5 G.

(12) Sheldrick, G. M. *SHELXTL, Crystallographic Software Package*, version 6.10; Bruker-AXS: Madison, WI, 2000.

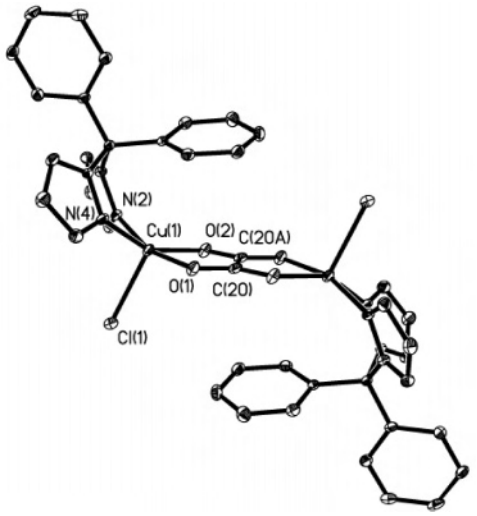

Figure 3. Structure of compound **1** with 50% thermal ellipsoids and hydrogen atoms omitted for clarity.

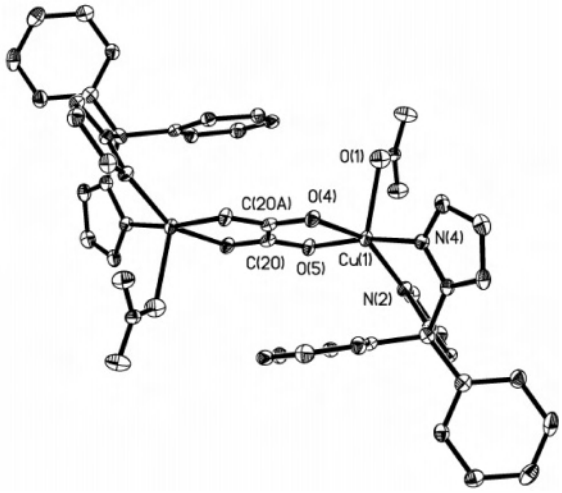

Figure 4. Structure of compound **2** with 50% thermal ellipsoids and hydrogen atoms omitted for clarity.

Magnetic Susceptibility. Magnetic susceptibility measurements were performed on a 7 T Quantum Design MPMS SQUID magnetometer. Measurements of magnetization as a function of temperature were performed from 1.8 to 300 K and in a 5000 G field. Samples were prepared by crushing single crystals to a fine powder. Approximately 15 mg samples were packed between cotton plugs, placed into gelatin capsules, cooled in zero applied field, and measured upon warming. Diamagnetic corrections were applied on the basis of Pascal's constants. Data of χT vs T were modeled by nonlinear least-squares fitting to the Bleaney−Bowers expression for two Cu^{2+} centers, including the usual term for the presence of uncoupled Cu^{2+} and temperature-independent paramagnetism where necessary. The data were corrected for the diamagnetism of the gel cap and the cotton plug.

Results and Discussion

The perspective views of compounds **1, 2**, and **4** are shown in Figures 3−5, crystallographic data are located in Table 1, and selected bond distances and angles are provided in

(13) Forrester, A. R.; Neugebauer, F. A. In *Landolt-Borstein: Magnetic properties of free radicals*; Fischer, H., Hellwege, K. H., Eds.; Springer Verlag: Berlin, 1979; Part C1.

Table 1. Crystallographic Data for Compounds **1**, **2**, and **4**

param	**1**	**2**	**4**
mol formula	$Cu_2Cl_2O_4C_{40}H_{32}N_8$	$Cu_2O_{10}C_{40}H_{32}N_{10}$	$Cu_2O_6C_{44}H_{44}N_8(N_2O_6)\cdot H_2O$
fw	886.74	939.84	1049.99
cryst system	triclinic	triclinic	monoclinic
space group	$P\bar{1}$	$P\bar{1}$	$C2/c$
cell constants			
a (Å)	8.6155(8)	8.863(7)	23.4588(14)
b (Å)	10.1435(9)	10.241(9)	8.8568(5)
c (Å)	11.3612(11)	11.425(10)	21.7818(13)
α (deg)	95.535(2)	98.985(14)	90
β (deg)	110.303(2)	110.449(13)	100.8890(10)
γ (deg)	106.111(2)	103.664(14)	90
Z	2	2	4
V (Å^3)	873.90(14)	911.1(13)	4444.1(5)
abs coeff μ_{calc} (mm^{-1})	1.428	1.247	1.036
δ_{calc} (Mg/m^3)	1.685	1.713	1.569
$R(F)$	0.0365	0.0555	0.0320
$R_w(F^2)$	0.0934	0.1168	0.0823
GOF	1.064	1.045	1.063

Table 2. Structures of all three complexes are very similar and will be discussed together to avoid redundancy.

The compounds consist of centrosymmetric $[Cu_2(Pz_2CPh_2)_2(X)_2(\mu\text{-}C_2O_4)]$ (X = Cl (**1**) NO_3 (**2**)) neutral entities or $[Cu_2(Pz^{3m}{}_2CPh_2)_2(H_2O)_2(\mu\text{-}C_2O_4)]^{2+}$ (**4**) cationic entities. In compounds **1**−**3** the axial ligand is a counteranion, but in **4** a water molecule is coordinated in the apical site and two noncoordinating nitrates exist in the crystal lattice for charge balance. Each copper(II) ion is in a 4 + 1 distorted square pyramidal coordination environment with two nitrogen atoms from the terminal ligand and two oxygen atoms from the bridging oxalate in the basal plane. The Cu−O_{ox} bond lengths are in the range 1.957(3)−2.011(3) Å with the two extreme lengths of this range both arising in compound **2**. The Cu−N bond lengths are in the range 1.959(3)−2.002(2) Å, and the Cu−Cu distances are in the range 5.130−5.212 Å (Table 2) which are typical for this class of compounds.[5]

The phenyl group of the DPDPM ligand partially shields the copper(II) ions preventing coordination of a sixth ligand to the metal centers and enforcing the square pyramidal

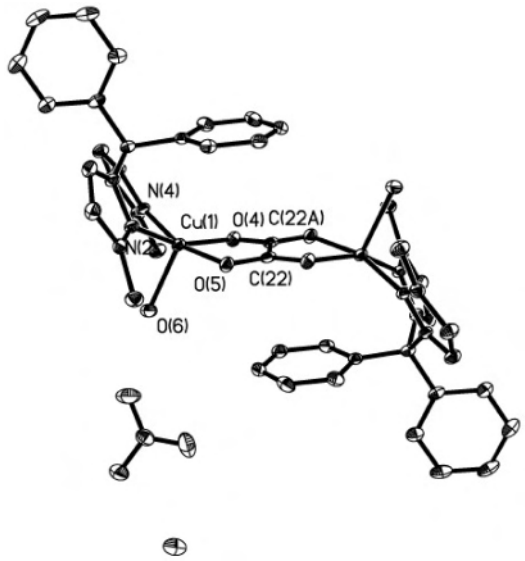

Figure 5. Structure of compound **4** with 50% thermal ellipsoids and hydrogen atoms omitted for clarity.

Table 2. Selected Bond Lengths (Å) and Angles (deg) for Compounds **1**, **2**, and **4**

	$[Cu_2(Pz_2CPh_2)_2(Cl)_2(\mu\text{-}C_2O_4)]$ (**1**)		
Cu−O1	1.9921(17)	N2−Cu−O1	162.21(8)
Cu−O2	2.0009(17)	N2−Cu−O2	90.25(7)
Cu−N2	1.991(2)	O1−Cu−O2	83.78(7)
Cu−N4	2.002(2)	N2−Cu−N4	85.39(8)
Cu−Cl	2.3961(7)	O1−Cu−N4	92.15(7)
O1−C20	1.257(3)	O2−Cu−N4	152.39(8)
C20−C20A	1.535(5)	N2−Cu−Cl	100.14(6)
Cu−Cu	5.212	O1−Cu−Cl	97.64(5)
		O2−Cu−Cl	108.27(5)
		N4−Cu−Cl	99.33(6)
	$[Cu_2(Pz_2CPh_2)_2(NO_3)_2(\mu\text{-}C_2O_4)]$ (**2**)		
Cu−O4	2.011(3)	N4−Cu−O5	168.53(11)
Cu−O5	1.957(3)	N4−Cu−O4	91.32(12)
Cu−N2	1.982(3)	O4−Cu−O5	84.55(11)
Cu−N4	1.959(3)	N2−Cu−N4	86.46(12)
Cu−O1	2.192(3)	O4−Cu−N2	151.01(12)
O5−C20	1.259(4)	O5−Cu−N2	91.97(11)
C20−C20A	1.540(7)	N4−Cu−O1	91.24(12)
Cu−Cu	5.161	O4−Cu−O1	88.55(12)
		O5−Cu−O1	99.33(12)
		N2−Cu−O1	120.36(12)
	$[Cu_2(Pz^{3m}{}_2CPh_2)_2(H_2O)_2(\mu\text{-}C_2O_4)](NO_3)_2\cdot H_2O$ (**4**)		
Cu−O4	1.9996(12)	N4−Cu−O5	162.84(5)
Cu−O5	1.9799(11)	N4−Cu−O4	89.08(5)
Cu−N2	1.9955(14)	O4−Cu−O5	84.06(5)
Cu−N4	1.9699(13)	N2−Cu−N4	90.18(6)
Cu−O6	2.1719(13)	O4−Cu−N2	157.66(5)
O5−C22	1.254(2)	O5−Cu−N2	90.24(5)
C22−C22A	1.540(3)	N4−Cu−O6	94.32(6)
Cu−Cu	5.178	O5−Cu−O6	102.54(5)
		O4−Cu−O6	103.01(5)
		N2−Cu−O6	99.32(5)

geometry. The shortest Cu−C_{phenyl} distances are in the range 3.031−3.163 Å for compounds **1**, **2**, and **4**. It has been shown in molybdenum complexes with DPDPM[9] that π-bonding interactions can occur between the phenyl ring and the metal center, but here there are no such observed interactions in our compounds.

In compounds **1**−**4** the oxalate bridges the two copper atoms in the very common symmetric bis(bidentate) fashion. In compounds **1** and **2** the oxalate bridge is essentially planar; however, the Cu−ox−Cu unit is not perfectly planar with copper deviations of ±0.121 and ±0.101 Å with respect to the mean plane of the oxalate dianion. The oxalate bite angles at copper for these two compounds are very similar

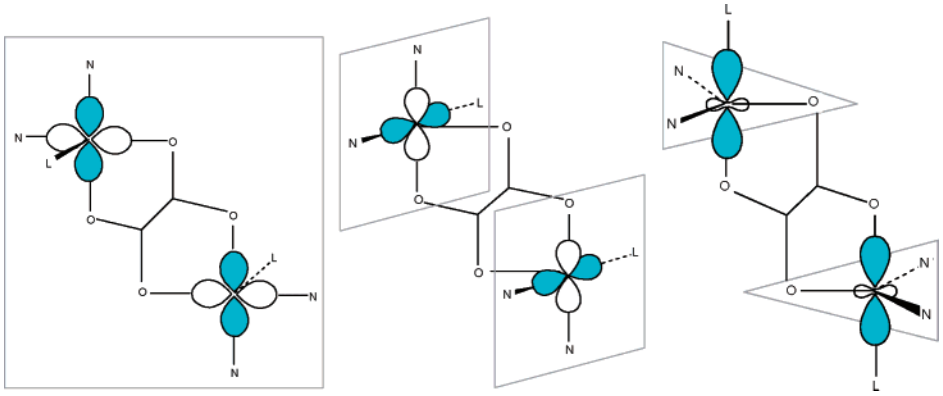

Figure 6. Common geometries and the magnetic orbitals used to describe bridged dinuclear copper(II) oxalate compounds: NNOO, left; NNLO, middle; TBP, right.[14]

(84.55(11)° (**1**) and 83.78(7)° (**2**)). In compound **4** the oxalate bridge is significantly distorted from planarity with carbon deviations of ±0.273 Å. In addition, the Cu−ox−Cu entity is not planar with copper deviations of ±0.266 Å. In compound **4** the bite angle of oxalate at copper is similar to that of compounds **1** and **2** with a value of 84.06(5)°. The planarity of this Cu−ox−Cu unit may affect the degree of overlap between the magnetic orbitals on copper(II) and the σ-orbitals of the oxalate dianion, thus affecting antiferromagnetic coupling.

To explain the degree of antiferromagnetic coupling in oxalato-bridged dinuclear compounds several structural parameters have been invoked in the literature. Variation in the degree of coupling has been primarily attributed the orientation of the semioccupied magnetic orbitals (SOMOs). SOMOs are defined as the half-filled highest occupied molecular orbitals (HOMOs) of the copper(II) d^9 metal ions.[14] For a five coordinate copper(II) center, the two possible geometries are square pyramidal and trigonal bipyramidal. For an N_2LO_2 coordination environment where N_2 is the DPDPM ligand, O_2 is the oxalate dianion, and L is the axial ligand, three SOMO orientations can be envisioned. Figure 6 shows the ideal geometries and the magnetic orbitals used to describe these coordination modes. These arrangements are named on the basis of their basal planes and can be called NNOO, NNLO, and TBP, respectively.

Compounds **1**−**4** fit the NNOO category with the magnetic orbitals of the copper(II) ions best described as $d_{x^2-y^2}$. In the literature, this configuration typically leads to the highest degree of antiferromagnetic coupling. The oxalate bridges the metal centers symmetrically, and the magnetic orbitals of the copper(II) ions are ideally situated for optimal overlap with the in-plane oxalate σ-orbitals. Therefore, compounds **1**−**4** should all exhibit strong antiferromagnetic coupling on the basis of the orientation of their SOMOs.

Simple parameters have been used in the literature to correlate the degree of antiferromagnetic coupling to the structures of oxalato-bridged dinuclear copper(II) compounds. The first of these, τ, developed by Addison et al.[15] can quantify variations in geometry from ideal tetragonal to ideal trigonal bipyramidal for five-coordinate copper(II) complexes. The formula used is $\tau = (\beta - \alpha)/60$, where β and α are the largest and second largest angles of the type L−Cu−L, surrounding the metal center ($\tau = 0$ for tetragonal geometry and $\tau = 1$ for trigonal bipyramidal geometry). Any deviations from ideal tetragonal geometry should decrease the overlap of magnetic orbitals with the σ-oxalate orbitals, thus decreasing the observed antiferromagnetic coupling. In addition, the degree of displacement of the copper(II) atom from the basal coordination plane (h_M),[14,16] and the dihedral angle formed between the basal plane and the oxalate bridging plane (γ) can also be considered.[14,16] A density functional calculation paper by Cano et al. proposes a correlation between these distortion parameters and magnetic exchange.[14] The apical ligand was chosen for study here because it is partially responsible for both of these distortions.

Tabulated below are the values for τ, h_M, and γ for compounds **1**−**4** and for several structurally similar compounds taken from the literature for comparison (Table 3). Values for τ vary significantly across the series with $\tau =$ 0.16 (**1**), 0.29 (**2**), 0.039 (**3**) (parameters for compound **3** are based on an isotropic solution of the twinned single-crystal data), and 0.086 (**4**). On the basis of this distortion from ideal tetragonal geometry, one would predict the antiferromagnetic exchange to increase on the order **2** < **1** < **4** < **3**. The parameter h_M follows the series **1** (0.39), **2** (0.35), **3** (0.26), and **4** (0.34). Although these numbers are very similar across the series, on the basis of this distortion, one would predict the magnetic exchange to increase in the order **1** < **2** ∼ **4** < **3**. Finally, the angle represented by γ is significant in compounds **1**, **2**, and **4** (18.7−23.6°) and much smaller in compound **3** (2.6°). This difference in γ for the series must result from the variation of the axial ligand and its interactions with the copper(II) ions. On the basis of γ, the coupling values should increase in the order **4** < **1** < **2** < **3**. All three of these predictions agree in the placement of compound **3** as the strongest antiferromagnetically coupled, but they differ in the order of the remaining three compounds.

Experimentally these predictions for the degree of antiferromagnetic coupling based on structural parameters can

(14) Cano, J.; Alemany, P.; Alvarez, S.; Verdaguer, M.; Ruiz, E. *Chem.*−Eur. J. **1998**, *4*, 476−484.

(15) Addison, A. W.; Rao, T. N.; Reedijk, J.; van Rijn, J.; Verschoor, G. C. *J. Chem. Soc., Dalton Trans.* **1984**, 1349−1356.

(16) Alvarez, S.; Julve, M.; Verdaguer, M. *Inorg. Chem.* **1990**, *29*, 4500−4507.

Table 3. Geometric Parameters for Compounds **1**−**4** and Several Selected Complexes with Similar Geometry Taken from the Literature for Comparison

	h_M	γ (deg)	τ	ref
$[Cu_2(Pz_2CPh_2)_2(Cl)_2(\mu\text{-}C_2O_4)]$ (**1**)	0.39	20.3	0.16	
$[Cu_2(Pz_2CPh_2)_2(NO_3)_2(\mu\text{-}C_2O_4)]$ (**2**)	0.35	18.7	0.29	
$[Cu_2(Pz_2CPh_2)_2(ClO_4)_2(\mu\text{-}C_2O_4)]$[a] (**3**)	0.26	2.6	0.039	
$[Cu_2(Pz^{3m}{}_2CPh_2)_2(H_2O)_2(\mu\text{-}C_2O_4)](NO_3)_2\cdot H_2O$ (**4**)	0.34	23.6	0.086	
$[Cu_2(tmen)_2(H_2O)_2(C_2O_4)](ClO_4)_2\cdot 1.25H_2O$[b]	0.15/0.18			0.14/0.11
$[Cu_2(mpz)_2(C_2O_4)(H_2O)_2](PF_6)_2\cdot mpz\cdot 3H_2O$[c]	0.24		0.13	17
$[Cu_2(bpy)_2(H_2O)_2C_2O_4][Cu(bpy)C_2O_4](NO_3)_2$[d]	0.15		0.09	5
$[Cu_2(bpy)_2(H_2O)_2C_2O_4][Cu(bpy)C_2O_4](ClO_4)_2$	0.18		0.18	5
$[Cu_2(bpy)_2(H_2O)_2C_2O_4][Cu(bpy)C_2O_4](BF_4)_2$	0.16		0.16	5
$[Cu_2(bpy)_2(H_2O)_2(NO_3)_2C_2O_4]$	0.11		NA	18

[a] Parameters based on an isotropic solution of single-crystal X-ray diffraction data. [b] tmen = *N,N,N′,N′*-tetramethylethylenediamine. [c] mpz = 4-methoxy-2-(5-methoxy-3-methylpyrazol-l-yl)-6-methylpyrimidine. [d] bpy = 2,2′-bipyridyl.

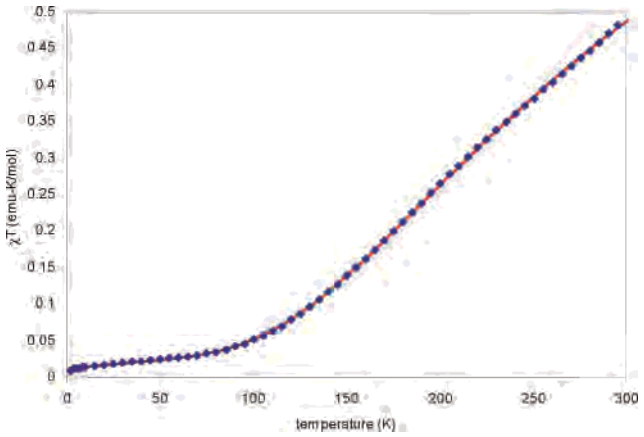

Figure 7. Plot of χT vs T and the fit to the Bleaney−Bowers expression for compound **4**.

be tested using variable-temperature magnetic susceptibility measurements. A representative plot of the product of molar susceptibility and temperature ($\chi_m T$) versus temperature (T) for compound **4** is given in Figure 7. As was expected on the basis of the NNOO $d_{x^2-y^2}$-type SOMO orientation, all four compounds exhibit behavior characteristic of strongly antiferromagnetically coupled copper(II) ions. It should be noted that these samples were difficult to measure because they are essentially diamagnetic at low temperatures. The data were successfully fit using a modified Bleaney−Bowers equation for coupled dinuclear copper(II) complexes starting with the Heisenberg Hamiltonian $H = -2JS_1S_2$.[19] The form of the expression used includes terms for uncoupled copper-(II) impurities and temperature-independent paramagnetism (TIP). The terms N, β, k, g, and T have their usual meanings, and ρ is the mole percent of paramagnetic impurity. A summary of the magnetic susceptibility parameters for all four compounds is tabulated below along with several structurally similar complexes selected from the literature for comparison (Table 4).

$$\chi T = \frac{2Ng^2\beta^2}{k\left[3 + \exp\left(-\frac{2J}{kT}\right)\right]}(1-\rho) + \frac{Ng^2\beta^2}{2k}\rho + (\mathrm{TIP})T \quad (1)$$

On the basis of the calculated values for $2J$, it is tempting to conclude that the structural parameter τ correctly predicts the ordering of magnetic exchange owing to the shift from tetragonal to trigonal bipyramidal geometry. The parameter h_M correlates fairly well with observed antiferromagnetic coupling, but the overall trend predicted by γ is not in agreement with the experimental data. However, the similarity of the $2J$ values for compounds **1, 2**, and **4** precludes any concrete correlations between these structural parameters and magnetic exchange. For compound **3**, where the $2J$ value is considerably higher than the others, these parameters correlate well with the observed coupling. The high degree of planarity at the copper(II) center indicated by the shortest h_M length, the smallest bending angle γ, and the lowest τ value should encourage increased antiferromagnetic coupling, and they do. Clearly the perchlorate anion is weakly bound, and this leads to one of the strongest instances of antiferromagnetic coupling for dinuclear oxalato-bridged copper(II) complexes that can be found in the literature.

In addition to temperature-dependent magnetic susceptibility, EPR spectroscopy can also provide an indication of the degree of communication between metal centers via hyperfine and superhyperfine coupling interactions, although such coupling does not always manifest. X-band EPR spectra of polycrystalline samples diluted with silica were collected at 105 K for all four compounds (Figure 8). In each case the signal is weak which therefore hinders interpretation.

Compound **2** has $g_{\|} = 2.24$ and $g_{\perp} = 2.08$ values and shows unresolved hyperfine splitting. The trend of $g_{\|} > g_{\perp}$ is indicative of a $d_{x^2-y^2}$-type orbital for the unpaired electron in a CuN_2O_2 chromophore. Compounds **1** and **4** exhibit four line hyperfine splitting patterns due to the Cu 3/2 nuclear spin. Values for $g_{\|}$ and $g_{\perp}$ were not distinguishable due to the broadness of the signals, but $g_{ave} = 2.09$ and 2.16 for **1** and **4**, respectively. In addition, the spectrum of compound **4** may also exhibit features of the triplet state along with g-anisotropy. The most interesting spectrum is observed for compound **3** which has a nine line splitting pattern. Hendrickson et al. report 7−14 line coupling patters in the EPR spectrum of the compound $[Cu_2(Me_5dien)_2(C_2O_4)](BPh_4)_2$ (where Me_5dien = 1,1,4,7,7-pentamethyldiethylenetriamine) which the authors believe result from interdimer magnetic

(17) Soto, L.; Garcia, J.; Escriva, E.; Legros, J. P.; Tuchagues, J. P.; Dahan, F.; Fuertes, A. *Inorg. Chem.* **1989**, *28*, 3378−3386.
(18) Castillo, O.; Muga, I.; Luque, A.; Gutiérrez-Zorrilla, J. M.; Sertucha, J.; Vitoria, P.; Román, P. *Polyhedron* **1999**, *18*, 1235−1245.
(19) Kahn, O. *Molecular Magnetism*; VCH: New York, 1993; p 107.

Table 4. Summary of Magnetic Susceptibility Parameters for Compounds **1**−**4** and Coupling Values for Several Selected Compounds Taken from the Literature for Comparison

	$2J^a$ (cm^{-1})	g^b	r	TIP	μ_{eff}(rt) (μ_B)	ref
$[Cu_2(Pz_2CPh_2)_2(Cl)_2(\mu\text{-}C_2O_4)]$ (**1**)	−364	2.24	0.031	*c*	1.90	
$[Cu_2(Pz_2CPh_2)_2(NO_3)_2(\mu\text{-}C_2O_4)]$ (**2**)	−344	2.16	0.013	1×10^{-3}	1.65	
$[Cu_2(Pz_2CPh_2)_2(ClO_4)_2(\mu\text{-}C_2O_4)]$ (**3**)	−424	2.12	0.032	2×10^{-4}	1.38	
$[Cu_2(Pz^{3m}{}_2CPh_2)_2(H_2O)_2(\mu\text{-}C_2O_4)](NO_3)_2 \cdot H_2O$ (**4**)	−378	2.23	0.013	2×10^{-4}	1.53	
$[Cu_2(tmen)_2(H_2O)_2(C_2O_4)](C\ lO_4)_2 \cdot 1.25\ H_2O$[d]	−385	2.16	0.0509			8d
$[Cu_2(mpz)_2(C_2O_4)(H_2O)_2](PF_6)_2 \cdot mpz \cdot 3H_2O$[e]	−402	2.18	0.005			17
$[Cu_2(bpy)_2(H_2O)_2C_2O_4][Cu(bpy)C_2O_4](NO_3)_2$[f]	−386	2.217				5a
$[Cu_2(bpy)_2(H_2O)_2C_2O_4][Cu(bpy)C_2O_4](ClO_4)_2$	−376	2.23				5a
$[Cu_2(bpy)_2(H_2O)_2C_2O_4][Cu(bpy)C_2O_4](BF_4)_2$	−378	2.20				5a
$[Cu_2(bpy)_2(H_2O)_2(NO_3)_2C_2O_4]$	−382	2.10	0.018			18

[a] All values have a standard deviation of ±2, and the correlation coefficient for each of the fits was 0.9999. [b] Values have a standard deviation of ±0.01. [c] Inclusion of the TIP term was not necessary to fit data for compound **1**. [d] tmen = *N*,*N*,*N*′,*N*′-tetramethylethylenediamine. [e] mpz = 4-methoxy-2-(5-methoxy-3-methylpyrazol-l-yl)-6-methylpyrimidine. [f] bpy = 2,2′-bipyridyl.

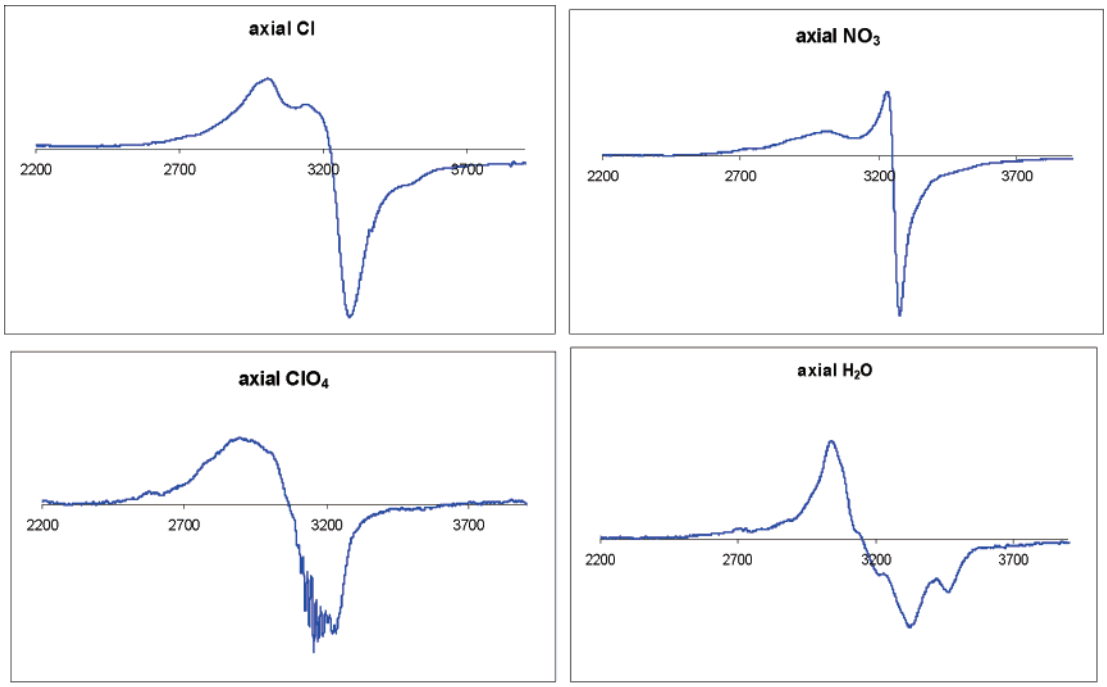

Figure 8. Solid-state X-band EPR spectra of $[Cu_2(Pz_2CPh_2)_2(Cl)_2(\mu\text{-}C_2O_4)]$ (**1**) (top, left), $[Cu_2(Pz_2CPh_2)_2(NO_3)_2(\mu\text{-}C_2O_4)]$ (**2**) (top, right), $[Cu_2(Pz_2CPh_2)_2(ClO_4)_2(\mu\text{-}C_2O_4)]$ (**3**) (bottom, left), and $[Cu_2(Pz^{3m}{}_2CPh_2)_2(H_2O)_2(\mu\text{-}C_2O_4)](NO_3)_2 \cdot H_2O$ (**4**) (bottom, right) at 105 K.

communiction.[20] However, the coupling constants observed for compound **3** are significantly smaller than those in Hendrickson's compound. The splitting in **3** most likely results from superhyperfine interactions between the four pyrazole nitrogen atoms across the oxalate bridge, resulting in a nine line pattern. This explanation is consistent with the high degree of planarity in compound **3** which places the nitrogen atoms close to the magnetic orbitals. Both interpretations are indicative of a highly planar, highly coupled dimer complex. Once again, the broadness and possible overlap of the signal inhibited obtaining individual $g_{||}$ and $g_{\perp}$values, but $g_{ave} = 2.12$. The data were examined for the forbidden dimer transition at half-field, but the signal intensity and the background of the silica dilutent hindered its detection.

(20) Felthouse, T. R.; Laskowski, E.; Hendrickson, D. N. *Inorg. Chem.* **1977**, *16*, 1077−1089.

Conclusion

We have begun to study the ligand diphenyldipyrazolylmethane and its coordination chemistry with copper(II) in oxalate-bridged dinuclear compounds to probe ligand−metal coupling interactions. By varying the donor ability of the axial ligand, we have slightly tuned the antiferromagnetic coupling between metal centers. All four compounds are strongly antiferromagnetically coupled. Structural parameters taken from the single-crystal X-ray data indicate that the parameter τ somewhat correlates structure with the degree of antiferromagnetic coupling. However, even in this small set of very structurally similar compounds, these simple parameters fail to provide any concrete predictive qualities. Future work will include the use of noncoordinating anions (i.e. triflate) to probe magneto−structural correlations.

Acknowledgment. J.L.S. acknowledges the GAANN fellowship for financial support. C.J.Z. acknowledges the

University of Akron for a faculty research grant (FRG-1524). G.T.Y. acknowledges the National Science Foundation (Grant CHE-023488) and the Virginia Tech ASPIRES program for each providing partial support for the purchase of the SQUID magnetometer. D.E.B and C.G. acknowledge Wayne State University.

Supporting Information Available: Magnetic susceptibility for compounds **1**−**3**, isotropic crystallographic refinement data tables for **3**, and crystallographic data in CIF format for compounds **1**, **2**, and **4**. This material is available free of charge via the Internet at http://pubs.acs.org.

IC048229T